The Ionization Constant of Water over Wide Ranges of Temperature and Density

Andrei V. Bandura

Department of Quantum Chemistry, St. Petersburg State University, 26 University Prospect, Petrodvoretz, St. Petersburg 198504, Russia

Serguei N. Lvov[a)]

The Energy Institute and Department of Energy & Geo-Environmental Engineering, The Pennsylvania State University, 207 Hosler Building, University Park, Pennsylvania 16802

(Received 26 April 2004; revised manuscript received 1 March 2005; accepted 5 April 2005; published online 8 December 2005)

A semitheoretical approach for the ionization constant of water, K_W, is used to fit the available experimental data over wide ranges of density and temperature. Statistical thermodynamics is employed to formulate a number of contributions to the standard state chemical potential of the ionic hydration process. A sorption model is developed for calculating the inner-shell term, which accounts for the ion–water interactions in the immediate ion vicinity. A new analytical expression is derived using the Bragg–Williams approximation that reproduces the dependence of a mean ion solvation number on the solvent chemical potential. The proposed model was found to be correct at the zero-density limit. The final formulation has a simple analytical form, includes seven adjustable parameters, and provides good fitting of the collected K_W data, within experimental uncertainties, for a temperature range of 0–800 °C and densities of 0–1.2 g cm^{-3}. © *2006 American Institute of Physics.* [DOI: 10.1063/1.1928231]

Key words: Bragg–Williams approximation; high temperatures and low densities; ionization constant of water; statistical thermodynamics solvation model.

Contents

Nomenclature. . . . 16
List of Symbols. . . . 16
1. Introduction. . . . 16
2. Theory and Computations. . . . 17
2.1. Thermodynamic Consideration. . . . 17
2.2. Model. . . . 17
2.2.1. Cavity Formation Energy. . . . 18
2.2.2. Solvation Contributions. . . . 18
2.2.3. Electrostatic Polarization Term. . . . 20
2.3. Simplified Analytical Expression. . . . 20
2.4. Fitting Procedure. . . . 21
2.5. Choice of Experimental Data. . . . 22
2.5.1. Conductivity. . . . 22
2.5.2. Potentiometry. . . . 23
2.5.3. Calorimetry. . . . 23
3. Results and Discussion. . . . 24
4. Acknowledgments. . . . 27
5. Appendix. . . . 27
6. References. . . . 29

List of Tables

1. Empirical parameters calculated using Model I. . . 22
2. Empirical parameters calculated using Model II. . 22
3. References on the experimentally obtained K_W data used for estimating the empirical parameters given in Tables 1 and 2. . . . 24
4. Negative logarithm (base 10) of the ionization constant of water, K_W, calculated using Model II [Eq. (39)]. . . . 25

List of Figures

1. Contributions to the residual part of the standard chemical potential change, $\Delta\mu^R$, as a function of density at 400 °. . . . 20
2. Temperature–density distribution of the available experimental K_W data: . . . 24
3. Deviation of calculated lg K_W values from experimental data in supercritical and low-density regions at $0.08 \leqslant D \leqslant 1.00$ g cm^{-3} . . . 26
4. Deviation of calculated lg K_W values from the experimental data in high-density region at $1.0 \leqslant D \leqslant 1.2$ g cm^{-3} . . . 26
5. Temperature dependence of lg K_W at the saturated vapor pressure for $T \geqslant 200$ °C . . . 26
6. Temperature dependence of lg K_W at a constant density . . . 26
7. Density dependence of lg K_W at 400 °C (upper curves) and 800 °C (lower curves) . . . 27
8. Dependence of lg K_W from lg(D/g cm^{-3}) at 400 and 800 °C . . . 27

a)Corresponding author; electronic mail: lvov@psu.edu

9. Bragg–Williams sorption isotherm, $\theta=\theta(z)$, calculated using different values of $\omega/RT=5$ (left curves) and $\omega/RT=30$ (right curves) 28
10. Excess chemical potential $\Delta\tilde{\mu}$ of the sorbent particle in the Bragg–Williams approximation calculated using different values of $\omega/RT=5$ (left curve) and $\omega/RT=30$ (right curve) 28

Nomenclature

Abbreviations

BMCSL	Boublik–Mansoori–Carnahan–Starling–Leland
M&F	Marshall and Franck
MSA	mean spherical approximation

List of Symbols

Symbol	Physical quantity	Unit
D	mass density	$g\,cm^{-3}$
f	fugacity	MPa
G	Gibbs energy	
K	ionization constant	
k	Boltzmann's constant	
l. u.	decimal logarithmic unit	
M	molar mass	$g\,mol^{-1}$
n	ion coordination number	
P	pressure	MPa
R	gas constant ($8.31451\,J\,mol^{-1}\,K^{-1}$)	
r	particle radius	Å
T	absolute temperature	K
V	volume	
v	molecular free-volume parameter	
z	sorption isotherm parameter	
ε	interparticle interaction parameter; relative permittivity	
ζ	particle diameter ratio	
η	reduced density	
θ	occupation fraction in solvation complex	
λ	absolute activity	
μ	chemical potential	
Ξ	grand partition function	
ρ	number particle density	
σ	parameter for interaction between solvation complex and bulk	
ω	water–water interaction energy in solvation complex	

Subscripts and superscripts

°	standard state (pure fluid for water and $1\,mol\,kg^{-1}$ solution exhibiting infinitely diluted properties for ionic species)
B	boundary between solvation complex and bulk
C	cavity
E	electrostatic polarization
G	ideal gas state
I	ion
R	residual part of the chemical potential
S	solvation complex
W	water
X	chemical component

1. Introduction

The standard-state thermodynamic properties of aqueous ions and molecules over wide ranges of temperature and density are required for modeling most of the physicochemical processes in aqueous media related to a number of important applications. The ionization constant of water (K_W) is a benchmark property in aqueous solution chemistry and K_W has been experimentally obtained over wide ranges of temperature and pressure (see a brief review of published papers below). In 1981, Marshall and Franck (M&F) proposed an empirical equation for pK_W, which was an empirical approach based on the available experimental measurements (Marshall and Franck 1981). The M&F equation has a simple analytical form and well represents the experimental data for densities above $0.4\,g\,cm^{-3}$. While the M&F equation, technically, allows an extrapolation below $0.4\,g\,cm^{-3}$, there is some concern (Chen *et al.* 1994a) that the M&F formulation may not give accurate values of K_W at low densities.

Several attempts have been made for predicting the standard chemical potentials of aqueous electrolytes at conditions other than ambient and most of the approaches have employed the well-known Born (1920) equation for estimating the continuum dielectric polarization by an ion. An improvement of this approximation led to the so-called semicontinuum models where the solvent in the region neighboring the ion is treated as a medium with discrete molecules, while the outside of this region is considered as a dielectric continuum (see, for example, Fernández-Prini *et al.* 1992). The semicontinuum models have been successful in a number of respects but cannot be used alone for calculating the ionization constant of water over a wide range of densities. In 1982, Pitzer made an attempt to calculate the ionization constant of water at high temperatures and low densities (Pitzer 1982). He regarded water vapor as a near-perfect gas mixture of hydrates of different compositions and used a reliable set of mass spectrometry data obtained by Kebarle (1977) and Lau *et al.* (1982). It was found that K_W values predicted by Pitzer decrease much faster than that obtaned from the M&F equation at densities below $0.4\,g\,cm^{-3}$, and the difference between M&F's and Pitzer's calculations can be up to 10 orders of magnitude. Tanger and Pitzer (1989a, b) extended the Pitzer's approach to a region of higher temperatures and densities to permit predictions up to 1000 °C and 500 MPa. The revised semicontinuum model of Tanger and Pitzer is a more realistic representation of both the inner-shell and outer-shell contributions to the hydration process. These authors concluded that their semicontinuum model is more reliable than the M&F equation at pressures and temperatures where the density of water is less than $0.4\,g\,cm^{-3}$.

Klots (1984) derived an equation for calculating the pH values of steam along the coexistence curve with liquid phase using a rather different approach than that of Tanger and Pitzer (1989a, b). Klots considered a distribution of ion–water clusters in the framework of a liquid-drop model. The author concluded that any extrapolation using the M&F equation might overestimate the ionic content of vapor at low temperatures and densities.

The paper of Tawa and Pratt (1995) should also be mentioned here as an example of the continuum approach. The authors have applied a dielectric solvation model to predict the equilibrium ionization of liquid water over wide ranges of density and temperature. In addition, the model includes an approximate description of the polarizability of dissociated water molecules. It was found that the calculated pK_W values are extremely sensitive to the water molecule radius, which is an adjustable parameter and was used to fit the experimental pK_W data.

In this paper, we present a new semitheoretical approach to fit the available experimental data of pK_W over wide ranges of water density (from 0 to 1.2 $g\,cm^{-3}$) and temperature (from 0 to 800 °C). Our model is based on a number of novel achievements in statistical mechanics applied to discrete molecular systems. It should be noted that our goal was not to develop a model to theoretically predict the ionization constant of water, but we derived a set of analytical expressions for reproducing and extrapolating the available experimental data to a region of low densities and high temperatures taking into account that the ideal gas K_W.

2. Theory and Computations

2.1. Thermodynamic Consideration

The ionization constant of water can be attributed to the following reaction: $2H_2O \Leftrightarrow H_3O^+ + OH^-$. Because the proton hydration is completed under all conditions of practical interest, we assume that this reaction may be used as a representative model for both liquid and vapor phases up to the zero density limit. The negative decimal logarithm of the ionization constant, pK_W, is defined as change of the standard Gibbs energy $[\Delta_W G^\circ(T,P)]$ divided by $RT\ln(10)$:

$$-RT\ln(10)pK_W = RT\ln K_W(T,P) = -\Delta_W G^\circ(T,P) = 2\mu_W^\circ(T,P) - 2\mu_I^\circ(T,P), \quad (1)$$

where $\mu_W^\circ(T,P)$ is the standard chemical potential of pure water and $\mu_I^\circ(T,P)$ is the mean ionic standard chemical potential of H_3O^+ and OH^-. Here and below we use the molal scale standard state for the ionic species, if not stated otherwise.

Generally, the chemical potential μ_X of a species X at a certain particle density, ρ_X, can be represented as a sum of the chemical potential of this species in the ideal gas state at the same temperature and density, $\mu_X^G(T,\rho_X)$, and the residual chemical potential, $\mu_X^R(T,\rho_X)$, as follows:

$$\mu_X(T,\rho_X) = \mu_X^G(T,\rho_X) + \mu_X^R(T,\rho_X). \quad (2)$$

The ideal gas chemical potential $\mu_X^G(T,\rho_X)$, can be calculated using the well-known statistical thermodynamic approach (Hill 1956)

$$\mu_X^G(T,\rho_X) = -RT\ln(q_X/\Lambda_X^3\rho_X) = \mu_X^{\circ G}(T) + RT\ln(x_X P^G/P_0), \quad (3)$$

where q_X is the intrinsic (vibrational) partition function, Λ_X is the kinetic (translational and rotational) partition function, x_X is the mole fraction of the component X, and P^G is the total pressure for the gas-phase reference system. $\mu_X^{\circ G}(T)$ in Eq. (3) is the gas-phase standard chemical potential, which can be presented as:

$$\mu_X^{\circ G}(T) = -RT\ln(kTq_X/\Lambda_X^3 P_0), \quad (4)$$

where P_0 is the standard pressure (0.1 MPa). It should be noted that the residual part of the chemical potential of X at density D ($g\,cm^{-3}$) is easily available because of the simple thermodynamic relation to the fugacity, f_X (MPa):

$$\mu_X^R(T,D) = -RT\ln(DRT/M_X f_X). \quad (5)$$

Introducing the terms that take into account the standard state corrections (Ben-Naim 1987), we can obtain the following expression for the water and ionic standard chemical potentials as:

$$\mu_W^\circ(T,D) = \mu_W^R(T,D) + \mu_W^{\circ G}(T) + RT\ln(DRT/M_W P_0), \quad (6)$$

$$\mu_I^\circ(T,D) = \mu_I^R(T,D) + \mu_I^{\circ G}(T) + RT\ln(DRT/M_W P_0) + RT\ln(M_W/10^3), \quad (7)$$

where D is the density of pure water, $\mu_I^{\circ G}(T)$ and $\mu_W^{\circ G}(T)$ are, respectively, the standard chemical potentials of ions and water molecules in the ideal gas state. Using Eqs. (6) and (7), Eq. (1) can be rewritten in a form which is convenient for representing the equilibrium constant of the ionization reaction in the ideal gas phase, $K_W^G(T)$ as:

$$RT\ln K_W(T,D) = 2\,\Delta\mu^R(T,D) + RT\ln K_W^G(T) - 2RT\ln(M_W/10^3), \quad (8)$$

where

$$\Delta\mu^R(T,D) = \mu_I^R(T,D) - \mu_W^R(T,D) \quad (9)$$

is the change of residual chemical potential of ion relative to that of the water molecule.

2.2. Model

Using the available thermodynamic reference data, the right-hand terms in Eq. (8) can be calculated except for the residual part of the chemical potential, $\Delta\mu^R(T,D)$. We assume that $\Delta\mu^R(T,D)$ can be considered as an average value for both ions H_3O^+ and OH^- and can be represented by three main contributions as follows: (1) $\Delta\mu^C$ is due to a cavity formation, (2) $\Delta\mu^S$ is due to short-range interactions within the first solvation sphere of an ion together with the interactions between molecules of the first solvation sphere

and the neighboring molecules of the surrounding bulk solvent, and (3) $\Delta\mu^{E}$ is due to electrostatic polarization of water beyond the solvation complex. Thus, $\Delta\mu^{R}(T,D)$ can be written as follows:

$$\Delta\mu^{R}(T,D)=\Delta\mu^{C}(T,D)+\Delta\mu^{S}(T,D)+\Delta\mu^{E}(T,D). \tag{10}$$

The hypothetical physical processes corresponding to each contribution to $\Delta\mu^{R}(T,D)$ are briefly described below.

We assume that in the first stage a cavity is created and it is large enough for imbedding an ion together with the first solvation sphere. Then, during the second stage, a certain number (not constant) of water molecules is transferred from the bulk water to the cavity. The short-range ion–water interaction forces are simultaneously turned on without any direct interaction between the ion and the outside cavity fluid. At the same time, the structure and energy changes should occur in the water molecules, which are closely bound to the solvation complex. Finally, the third stage occurs when the long-range polarization forces are taken into account in an interaction between the complex and bulk solvent. All of these processes are supposed to occur at the same pressure and temperature. To ascribe the statistical–thermodynamic relation to each contribution and to find the semiempirical expressions for them we consider the grand partition functions of the infinitely diluted solution (containing a single ion) and of the pure water. To provide the symmetry in equations to be derived, we also cut out (formally) the spherical cavity in the case of the pure water which surrounds a single fixed water molecule and contains the same number of molecules (on average) as coordinated by the ion. The representation of water molecules in pure fluid is the main difference between the present model and our previous consideration (Bandura and Lvov 2000). In accord with dividing the total space occupied by solution or bulk fluid we suppose that the total grand partition functions can be represented as a product of partition functions of two separated areas. Then, taking into account the fixed positions of the central particles and assuming that their intrinsic partition functions q_X are the same as in ideal gas in both cases, we can write:

$$\frac{\Xi_{SC}\Xi_{CI}}{\Xi_{FC}\Xi_{CW}}\exp\left(\frac{\Delta\mu^{R}}{RT}\right)=\exp\left(\frac{P(V_S-V_F)N_A}{RT}\right), \tag{11}$$

where Ξ_{SC}, Ξ_{FC}, Ξ_{CI}, and Ξ_{CW} are, respectively, the grand partition functions of the outside cavity fluids in solution and in pure water, solvation complex, and water molecules inside the cavity in pure water. The V_S and V_F are the total volumes of the solution and bulk fluid under the external pressure P, so $N_A(V_S-V_F)$ is the difference between partial molar volume of ion and that of the water molecule (N_A is Avogadro's number).

2.2.1. Cavity Formation Energy

Equation (11) can be rewritten as follows:

$$\Delta\mu^{R}=-RT\ln\left(\frac{\Xi_{SC}}{\Xi_{FC}}\right)+P(V_S-V_F)N_A-RT\ln\left(\frac{\Xi_{CI}}{\Xi_{CW}}\right). \tag{12}$$

The sum of the first two terms on the right-hand side of Eq. (12) can be interpreted as the $\Delta\mu^{C}+\Delta\mu^{E}$. Indeed, in the limit of the very large neutral cavities with the volumes V_{CI} and V_{CW} we have:

$$\begin{aligned}&-RT\ln\left(\frac{\Xi_{SC}}{\Xi_{FC}}\right)+P(V_S-V_F)N_A\\&=N_AP[-(V_S-V_{CI})+(V_F-V_{CW})+(V_S-V_F)]\\&=N_AP(V_{CI}-V_{CW})=\Delta\mu^{C}.\end{aligned} \tag{13}$$

In the presence of a charged ion in the cavity center, the free energy $\Delta\mu^{E}$ of the electrostatic polarization of water beyond the cavity must be added (see Sec. 2.2.3).

For estimating the cavity formation term we used the Boublik–Mansoori–Carnahan–Starling–Leland (BMCSL) expression (Lee 1988) that was obtained for hard-sphere fluids. This contribution depends only on the fluid density and radii of species

$$\begin{aligned}\mu^{C}(T,D,r_C)=RT\Bigg[&2\frac{\eta\zeta^3}{(1-\eta)^3}+3\frac{\eta\zeta^2}{(1-\eta)^2}\\&+3\frac{\eta\zeta(1+\zeta-\zeta^2)}{(1-\eta)}-(1-3\zeta^2+2\zeta^3)\\&\times\ln(1-\eta)\Bigg],\end{aligned} \tag{14}$$

where $\eta=(4\pi/3)\rho r_W^3$, $\zeta=r_C/r_W$, r_W is the hard sphere radius of water molecule, r_C is the cavity radius, and ρ is the number density of pure water, $\rho=N_AD/M_W$. The contribution $\Delta\mu^{C}$ in Eq. (10) can be calculated as a difference between the Gibbs energy of formation of the cavity around an ion in solution and the cavity around a single water molecule in the pure fluid:

$$\Delta\mu^{C}(T,D)=\mu^{C}(T,D,r_{CI})-\mu^{C}(T,D,r_{CW}), \tag{15}$$

where r_{CI} and r_{CW} are the appropriate radii.

2.2.2. Solvation Contributions

The last term on the right-hand side of Eq. (12) can be interpreted as $\Delta\mu^{S}$—solvation contribution to the residual part of the chemical potential change:

$$\Delta\mu^{S}=\mu_I^{S}-\mu_W^{S}, \tag{16}$$

$$\mu_I^{S}=-RT\ln(\Xi_{CI}), \tag{17}$$

$$\mu_W^{S}=-RT\ln(\Xi_{CW}). \tag{18}$$

In the literature, there is no rigorous analytical expression for the contribution that is responsible for the short-range interactions between an ion and water molecules. Therefore,

we will obtain a semiempirical equation for the short-range solvation using a quasilattice approach and the Bragg–Williams approximation (Hill 1956). In this approach an ion will be considered as a sorption center. By applying the quasilattice approach and the Bragg–Williams approximation, we can present Ξ_{CW} as:

$$\Xi_{CW}=\sum_{i=0}^{n}\frac{n!}{i!(n-i)!}z^i\exp(-i^2cw/2nRT), \quad (19)$$

where c is the number of nearest neighbors of a molecule within the first solvation shell, and w is the mean pair interaction energy per mole. It should be noted that w must be positive for a solvation process. This is because the increase of water molecules in the first solvation sphere of an ion reduces the stepwise gain in the solvation Gibbs energy (Kebarle 1977). The quantity z depends on the water absolute activity λ_W, the mean ion–molecular interaction energy ε_{CI} (per mole), and v_{CI}—the so-called free volume for water molecule in the solvation complex. Assuming that the intrinsic partition function of a water molecule in the solvation complex is the same as in pure water, we can write:

$$z=\rho\exp\left[-\frac{(\varepsilon_{CI}+\varepsilon_{CB}-RT\ln v_{CI}-\mu_W^R)}{RT}\right]. \quad (20)$$

The additional parameter ε_{CB} in Eq. (20) takes into account the interactions between molecule in the first solvation sphere and the neighboring molecules of the surrounding bulk solvent. It should be mentioned that all quantities in Eq. (20) depend on the properties of pure water. In the limit of low densities the quantity ε_{CI} should be on the order of $-100\ \mathrm{kJ\ mol^{-1}}$ as was found by treating the gas-phase mass spectrometry data (Kebarle 1977; Lau *et al.* 1982). The upper bound of v_{CI} can be roughly estimated as the volume of one cell V_{CI}/n.

An approximate evaluation of the sum in Eq. (19) in the limit of large n gives (Hill 1956; Lopatkin 1983)

$$\mu_I^S=nRT\left[\ln(1-\theta)-\frac{\omega\theta^2}{2RT}\right], \quad (21)$$

where $\omega=cw$, and θ is the occupation fraction of an ion solvation sphere. The value of θ is connected to the mean solvation number $\bar{n}$ by a relation: $\bar{n}=\theta n$. The dependence of θ on z is expressed by the well-known sorption isotherm (Hill 1956; Lopatkin 1983):

$$z=\theta(1-\theta)^{-1}\exp(\omega\theta/RT). \quad (22)$$

Employing Eq. (22), one can obtain another form of Eq. (21) as:

$$\mu_I^S=nRT\left[\theta\ln\frac{\theta}{z}+(1-\theta)\ln(1-\theta)+\frac{\omega\theta^2}{2RT}\right]. \quad (23)$$

It is a surprising fact (as shown in the Appendix), that a macroscopic approximation [Eqs. (21)–(23)] reproduces an exact result for $n\geqslant 6$, which can be obtained by direct summation in Eq. (19). Unfortunately, Eq. (22) cannot be analytically solved with respect to θ. Nevertheless, an explicit expression for $\theta(z)$ would be useful. For this purpose we have developed (see the Appendix) an approximate expression for θ which correctly reproduces the dependence of θ and $\partial\theta/\partial\ln z$ from z in the entire range of z from 0 to ∞ for sufficiently large and positive ω ($>5RT$) as follows:

$$\theta=\Theta(z)=\frac{1}{2}+\frac{1}{\omega/RT+4}\ln\left\{\frac{\cosh[\ln(z)/2+1]}{\cosh[\ln(z)/2-\omega/2RT-1]}\right\}. \quad (24)$$

It should be mentioned that at the point where $z=\exp(\omega/2RT)$, Eq. (24) gives the exact value of $\theta=1/2$. It was also found that Eq. (23) together with Eq. (24) can correctly reproduce the limiting behavior of μ_I^S at $\ln z\to-\infty(\theta\to 0)$ and $\ln z\to+\infty(\theta\to 1)$. Because of these features of Eqs. (23) and (24), we used an analytical expression for μ_I^S, which can be obtained by substituting Eq. (24) into Eq. (23). The resulting expression accurately reproduces both the exact summation using Eqs. (17) and (19) and the macroscopic approximation given by Eq. (21). Note that, as shown in the Appendix, these two approaches also give very close results.

Due to strong ion–water interactions in the solvation complex, θ appears to be appreciably less than 1 only at low densities. At high densities, where the experimental dissociation constants are available, θ is close to 1. In such a case Eq. (23) turns into a more simple expression:

$$\mu_I^S=-nRT(\ln z-\omega/2RT). \quad (25)$$

Therefore, Eq. (23) can be used for the correct extrapolation of available experimental K_W data to the low density and high temperature regions.

A simple adsorption model cannot be used for estimation of μ_W^S in Eq. (18) because interactions of water molecules within the cavity with the molecule in its center and between themselves are the same as the water–water interactions in the rest bulk fluid. However, taking into account the approximate nature of our equations, it is desirable to represent the $\bar{n}$ water molecules in the pure water ($\bar{n}=\theta n$) using the same level of approximations as it was done for $\bar{n}$ water molecules in the solvation complex. The simplest way to do this is to replace the grand partition function Ξ_{CW} in Eq. (18) by the canonical partition function with the fixed number of water molecules:

$$\Xi_{CW}=\left\{\exp\left[-\frac{(\varepsilon_{CW}-RT\ln\rho v_{CW}-\mu_W^R)}{RT}\right]\right\}^{\theta n}. \quad (26)$$

Here, as previously, we use the formal "free-volume" approach: the quantity ε_{CI} is the mean interaction energy of water molecules and v_{CW} is the free volume for water molecules within the regarded cavity. In the limit of low densities parameter v_{CW} tends to $1/\rho$, so the product ρv_{CW} is finite and nonzero at all densities.

By using Eqs. (23)–(25), an effective parameterization scheme should be developed. Below is a description of the empirical approach which was found to be sufficiently successful. Note that the derived equations cannot be considered as strict, and statistical mechanics was used to provide the correct limiting behavior at low densities.

We assume that quantities ε_{CI} and v_{CI} in Eq. (20) can be regarded as the constant empirical parameters. Following an assumption (Ono and Kondo 1960) we suppose that "surface" contribution ε_{CB}, in Eq. (20) should be proportional to $\rho^{2/3}$ and can be expressed using a single empirical constant σ_{CI}:

$$\varepsilon_{CB}=4\pi r_{CI}^2\sigma_{CI}\rho^{2/3}T^{-1}. \tag{27}$$

The factor $4\pi r_{CI}^2$ takes into account an area of the boundary surface between the bulk fluid and the cavity. Substituting Eq. (27) into Eq. (20), we have

$$z=\rho\exp\left[-\frac{(\varepsilon_{CI}-RT\ln v_{CI}+4\pi r_{CI}^2\sigma_{CI}\rho^{2/3}T^{-1}-\mu_W^R)}{RT}\right]. \tag{28}$$

For the parameter ω we have also adopted an inverse temperature dependence as

$$\omega=\omega_{CI}T^{-1}, \tag{29}$$

where ω_{CI} is the empirical constant.

It is known (Hill 1956; Lopatkin 1983) that the mean interaction energy between water molecules in bulk fluid should be proportional to density. We applied this assumption to reproduce the terms in Eq. (26) and adopt the following tree-parametric expression:

$$\varepsilon_{CW}-RT\ln\rho v_{CW}=\rho^{\gamma}(\varphi_{CW}-RT\,\psi_{CW}), \tag{30}$$

where φ_{CW} and Ψ_{CW} are the empirical constants. It was found that $\gamma=1/2$ provides a good fit of the experimental data. After these approximations, the final form of μ_W^S in Eq. (18) is as follows:

$$\mu_W^S=n\theta[\rho^{1/2}(\varphi_{CW}-RT\,\psi_{CW})-\mu_W^R]. \tag{31}$$

The last quantity that must be defined is the cavity size formed in bulk fluid which obviously depends on density. As it was stated above, this cavity contains a single central water molecule together with $\bar{n}$ water molecules around it at the bulk overall density. At a low fluid density the volume of this cavity V_{CW} can be approximated as $(4/3\pi r_W^3+\bar{n}/\rho)$. At a high density the volume should be close to the cavity volume V_{CI} in solution. The equation that we propose to use

$$V_{CW}=\frac{4}{3}\pi r_{CW}^3=n\left[\frac{\theta}{\rho}-\frac{\theta^\circ}{\rho^\circ}\right]+\frac{4}{3}\pi(r_{CW}^\circ)^3, \tag{32}$$

approximately satisfies both conditions. Here r_{CW}° is the radius of the cavity in liquid water at reference condition ($T_0=298.15$ K and $P_0=0.1$ MPa); and θ° and ρ° are, respectively, the occupation fraction of the solvation complex and density of water at reference condition. Note that θ° is supposed to be close to unity.

2.2.3. Electrostatic Polarization Term

The third term on the right-hand side of Eq. (10) adopts an analytical expression for the mixture of dipolar and ionic hard spheres based on the mean spherical approximation (MSA) (Garisto *et al.* 1983). This contribution depends on the ionic charge q, relative permittivity of solvent ε_W, and radius r_X, ($r_X=d_X/2$) of the solute molecules. According to Garisto *et al.* (1983)

$$\mu_I^E(T,D)=-\frac{1}{2}\left(1-\frac{1}{\varepsilon_W}\right)\frac{q^2}{r_{CI}+\Delta}, \tag{33}$$

where

$$\Delta=r_W\left[1-\frac{6b_0}{1+4b_0}\right], \tag{34}$$

and b_0 is defined by

$$\varepsilon_W=(1+4b_0)^2(1+b_0)^4(1-2b_0)^{-6}. \tag{35}$$

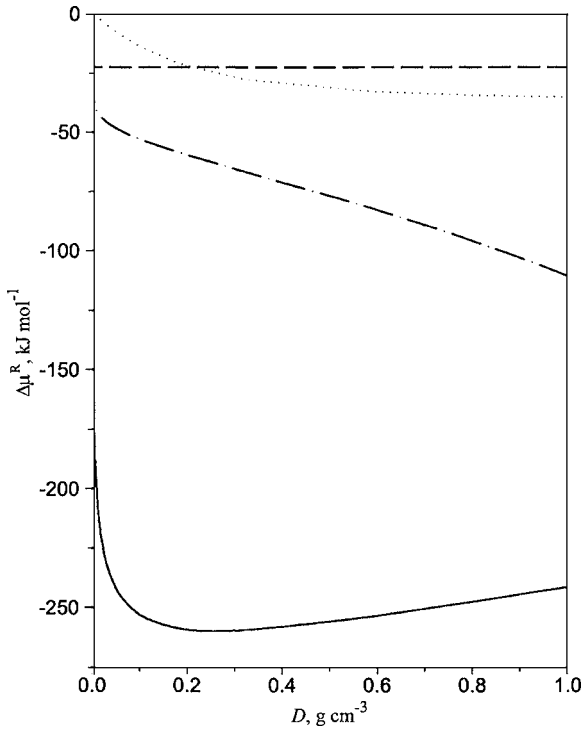

FIG. 1. Contributions to the residual part of the standard chemical potential change, $\Delta\mu^R$, as a function of density at 400 °C: (— — —) standard state correction, $\Delta\mu^\circ$; (–·–) cavity formation term, $\Delta\mu^C$; (—) contribution of the short-range solvation, $\Delta\mu^S$; (· · · ·) electrostatic contribution, $\Delta\mu^E$.

2.3. Simplified Analytical Expression

Our final set of expressions includes Eqs. (14)–(16), (23), (24), (28), (29), and (31)–(35) which describe the residual part contributions [Eq. (10)] of the standard ionic chemical potential change $\Delta\mu^R$. We will refer this set of equations as Model I. In Fig. 1 we plot the density dependence of the contributions $\Delta\mu^C$, $\Delta\mu^S$, and $\Delta\mu^E$, which has been calculated for an isotherm of 400 °C using the obtained empirical parameters (see below for details). As can be seen in Fig. 1, all calculated contributions are negative. The solvation term $\Delta\mu^S$, as expected, gives a dominant contribution, and a great deal of its value (~90%) is gained when water density rises from 0 to about 0.1 g cm^{-3}. The cavity formation term is also pronounced and its negative value is due to the fact that

water molecules occupy more space in pure water than in the solvation complex ($r_{CW} > r_{Cl}$). So, $\Delta\mu^C$ may be attributed to the water electrostriction that occurred around an ion. Because of the relatively large size of the solvation complex (≈ 4 Å) the electrostatic contribution is the smallest part and it varies slowly at $D > 0.4$ g cm^{-3}. This, in particular, means that the Born (1920) equation may be used instead of the MSA for evaluation of the electrostatic term. Assuming that the solvation term is the most important contribution, and other terms may be implicitly reproduced by empirical parameters, Eq. (8) can be rewritten in the following form:

$$\mathrm{p}K_W(T,D) = \frac{2}{RT\ln(10)}[\mu_I^S(T,D) - \mu_W^S(T,D)] + \mathrm{p}K_W^G(T) + 2\lg\frac{M_W}{10^3}. \quad (36)$$

Further simplifications are possible if we suppose that ω can be set to zero in Eqs. (21)–(23). In this case, the solvation term [Eqs. (20)–(23)] reduces to a simple Langmuir-like equation:

$$\mu_I^S = -nRT\ln(1+z); \qquad z = \rho\exp(-u/RT), \quad (37)$$

where u (and possibly n) is the empirical function of density and temperature. The bulk water contribution to $\Delta\mu^S$ also can be expressed by a simple equation containing the empirical function v, which depends on density and temperature:

$$\mu_W^S = n\theta\rho^\gamma v; \qquad \theta = \frac{z}{z+1}, \quad (38)$$

[see Eq. (31)]. It should be noted that functions u and v need not include the residual chemical potential of pure water μ_W^R due to mutual canceling of its contribution in μ_I^S and μ_W^S. Equations (36) and (37) may be used as a basis for the purely empirical fit of the ionization constants of water and other weak electrolytes.

In the present work we have applied the short form of equations described previously to simplify the results obtained by the entire set of equations of Model I. It was found that the following simple equation:

$$\mathrm{p}K_W(T,D) = -2n\left[\lg(1+Z) - \frac{Z}{Z+1}D(\beta_0 + \beta_1 T^{-1} + \beta_2 D)\right] + \mathrm{p}K_W^G(T) + 2\lg\frac{M_W}{10^3}; \quad (39)$$

$$Z = D\exp(\alpha_0 + \alpha_1 T^{-1} + \alpha_2 T^{-2} D^{2/3})$$

can accurately reproduce the observed K_W data with precision corresponding to experimental errors.

Note that the temperature dependence of the ionization constant $\mathrm{p}K_W^G(T)$ in the ideal gas state is easily available and will be considered below. Details of the fitting procedure and discussion of the results will also be given in the next sections. From here and below we will refer to Eq. (39) as Model II. Finally, we would like to show that the M&F equation (Marshall and Franck 1981)

$$-\mathrm{p}K_W^{M\&F}(T,D) = A(T) + B(T)\lg D, \quad (40)$$

where

$$A(T) = A_0 + A_1 T^{-1} + A_2 T^{-2} + A_3 T^{-3}$$

and

$$B(T) = B_0 + B_1 T^{-1} + B_2 T^{-2} \quad (41)$$

can be rewritten in the following form:

$$-\mathrm{p}K_W^{M\&F}(T,D) = -2N\lg(1 + De^{-U/RT}) + \mathrm{p}K_W^G(T) + 2\lg\frac{M_W}{10^3}, \quad (42)$$

which exhibits the correct limiting behavior when density is zero. We will call Eq. (42) the modified M&F equation. At a large density we can neglect unity compared to z in Eq. (37). In this case, combining Eqs. (36) and (40) and removing (for simplicity) the contribution of $\mu_W^S(T,D)$, we will have:

$$-2N\lg D + \frac{2NU}{RT\ln(10)} + \mathrm{p}K_W^G(T) + 2\lg\frac{M_W}{10^3} = -A(T) - B(T)\lg D. \quad (43)$$

Assuming that N and U are functions of temperature only, we can find that

$$N(T) = \frac{1}{2}B(T)$$

$$U(T) = -\frac{RT\ln(10)}{B(T)}\left[A(T) + \mathrm{p}K_W^G(T) + 2\lg\frac{M_W}{10^3}\right]. \quad (44)$$

Substituting N and U from Eq. (44) to Eq. (42) we can obtain modified form of M&F equation which coincides with the original form at sufficiently large densities and has the correct limit at $z \to 0$.

2.4. Fitting Procedure

Using Model I described above we have found that it is convenient to fit the deviation of $\mathrm{p}K_W$ from its standard value $\mathrm{p}K_W^0$ taken at a reference temperature of $T_0 = 298.15$ K, pressure of $P_0 = 0.1$ MPa, and density of D_0, which can be calculated from the equation of state of water. Therefore, Eq. (8) can be rewritten as follows:

$$\mathrm{p}K_W(T,D) = \frac{T_0}{T}\mathrm{p}K_W^0 + \frac{2}{RT\ln(10)}[\Delta\mu^R(T,D) - \Delta\mu^R(T_0,D_0)] + \mathrm{p}K_W^G(T) - \frac{T_0}{T}\mathrm{p}K_W^G(T_0) + 2\left(1 - \frac{T_0}{T}\right)\lg\frac{M_W}{10^3}. \quad (45)$$

By using Model I, we need to estimate (besides the empirical parameters): (1) the ideal gas ionization constant $K_W^G(T)$ and (2) the value of the residual water chemical potential $\mu_W^R(T,D)$. We calculated the ideal gas ionization con-

stant of water using JANAF98 data (Chase 1998) for the gas phase formation constants $\lg K_f(X)$ ($X=H_3O^+$, OH^-, H_2O),

$$pK_W^G(T) = 2\lg K_f(H_2O,T) - \lg K_f(H_3O^+,T) - \lg K_f(HO^-,T), \quad (46)$$

and then we approximated its temperature dependence by the function:

$$pK_W^G(T) = 0.61415 + 48251.33T^{-1} - 67707.93T^{-2} + 10102100T^{-3}. \quad (47)$$

The empirical coefficients in Eq. (47) were obtained using the least squares fitting procedure and the maximum error of such an approximation is about 0.001 logarithmic units (l. u.) at temperatures from 0 to 1000 °C.

A new formulation of thermodynamic properties of water and steam (Harvey *et al.* 2000; Wagner and Pruß 2002) was used for calculating the residual water chemical potential. We have directly employed Eq. (5) for obtaining the $\mu_W^R(T,D)$ values in Eq. (45).

Note that Model I provides the correct temperature dependence of $K_W(D,T)$ when $D \to 0$. However, the adopted fitting procedure does not allow estimating the absolute value of pK_W at $D=0$. Therefore, the standard value, $pK_W(0,T_0)$, has been included in Model I to ensure the correct limit at zero density. The $pK_W(0,T_0)$ value was calculated using JANAF98 (Chase 1998) gas phase Gibbs energies of formation and was found to be 158.58, including the standard state correction.

Our final expressions for Model I includes ten empirical parameters (n, r_W, r_{CI}, $\overset{\circ}{r}_{CW}$, ε_{CI}, υ_{CI}, σ_{CI}, ω_{CI}, φ_{CW}, and ψ_{CW}) that are to be estimated using the available experimental data. To reduce the number of these parameters, we will assume that the water molecule radius, r_W, can be presented as $r_{CI}/3$. This assumption looks reasonable if we take into account that the effective sizes of H_3O^+ and OH^- ions are close to that of the water molecule. The ion coordination number n was chosen to be 6. The remaining eight empirical parameters have been obtained using the nonlinear least squares fitting procedure and employing a large array (237 points) of experimental data as described below. In the fitting procedure we have taken into account the weights of all experimental points. Each weight was calculated as the inverse square of the reported or estimated experimental error. The standard deviation of the nonlinear least-square fitting was found to be 0.16 l. u. The calculated empirical parameters are given in Table 1. The obtained values of the cavity radii $r_{CI}=3.9$ Å, $\overset{\circ}{r}_{CW}=4.4$ Å, and the water molecule radius $r_W=1.3$ Å, all look reasonable. Also, the value of ε_{CI} was found to be $-70\ \mathrm{kJ\,mol^{-1}}$. This parameter represents the mean linear increment of the gas phase solvation enthalpies upon successive hydration of H_3O^+ and OH^-. Using the gas-phase mass spectrometry data (Kebarle 1977; Lau *et al.* 1982), a value of about $-100\ \mathrm{kJ\,mol^{-1}}$ can be found and it is quite close to the figure estimated above.

TABLE 1. Empirical parameters calculated using Model I

No.	Parameter	Value	Units[a]
1	n	6[b]	—
2	r_{CI}	3.93407	Å
3	$\overset{\circ}{r}_{CW}$	4.39515	Å
4	ε_{CI}	−70.1901	kJ mol^{-1}
5	υ_{CI}	8.51597	Å^3
6	σ_{CI}	−26.4898	kJ mol^{-1} K
7	ω_{CI}	1479.20	kJ mol^{-1} K
8	φ_{CW}	−18.8466	kJ mol^{-1} Å$^{3/2}$
9	ψ_{CW}	18.7534	Å$^{3/2}$

[a]1 Å = 0.1 nm.
[b]Value of n was taken as a constant in estimating the empirical parameters.

To apply Model II [Eq. (39)] at a fixed temperature and density we need to know only seven empirical parameters: n, α_0, α_1, α_2, β_0, β_1, β_2 besides Eq. (47) for the ideal gas ionization constant of water. For estimating these parameters, we have used the same set of experimental data and generally the same adjusting procedure as was applied for Model I. As previously, we set the ion coordination number n equal to 6. The only difference in constructing Model II was that we fit the values of pK_W directly without reference to the standard value, $pK_W(0,T_0)$. The obtained values of n, α_0, α_1, α_2, β_0, β_1, and β_2, are given in Table 2. The standard deviation of the nonlinear least-square fitting was 0.16 l. u., which is the same as in Model I. Moreover, the difference between the two models was found to be very small and the standard deviation of Model II from Model I was less than 0.05 l. u. Therefore, in most of the figures (except that showing the experimental data deviations) we demonstrate the results using Model II.

2.5. Choice of Experimental Data

Three main experimental techniques have been used for measuring the ionization constant of water over wide ranges of temperature and pressure: (1) conductivity, (2) potentiometry, and (3) calorimetry.

2.5.1. Conductivity

Measurement of the electrical conductivity is one of the most convenient methods for determining the dissociation/association constants of aqueous electrolytes. By obtaining the conductances of a series of dilute solutions of a weak

TABLE 2. Empirical parameters calculated using Model II

No.	Parameter	Value	Units
1	n	6[a]	—
2	α_0	−0.864671	—
3	α_1	8659.19	K
4	α_2	−22786.2	(g cm^{-3})$^{-2/3}$ K^2
5	β_0	0.642044	(g cm^{-3})$^{-1}$
6	β_1	−56.8534	(g cm^{-3})$^{-1}$ K
7	β_2	−0.375754	(g cm^{-3})$^{-2}$

[a]Value of n was taken as a constant in estimating the empirical parameters.

acid (or base) and its salt, the ionization constant of water can be obtained. Historically, the high-temperature conductivity studies were initiated by Noyes *et al.* (1910). The authors were able to achieve a relatively high accuracy comparable to that which can be obtained in modern observations. However, the extrapolation method, used in that study for obtaining the limiting values, was different and is not suitable at the present time. Because of a significant difference in the data treatment, we did not include the data of Noyes *et al.* (1910) in the fitting procedure. Fortunately, most of the latest works were based on relatively modern solution theories (Robinson and Stokes 1965). For example, the Shedlovsky equation and its modifications were extensively used to obtain the limiting conductance. The Debye–Hückel theory was also applied to calculate the activity coefficients. Since the early 1960s, Quist and Marshall have carried out extensive conductivity measurements for a variety of aqueous electrolyte solutions, mostly at temperatures from 400 to 800 °C and pressures up to 400 MPa (Quist and Marshall 1968). Quist (1970) measured the electrical conductance of aqueous NH_4Br in the supercritical region and accomplished the investigations that allowed estimating K_W. The conductivity data of NH_4Br solutions were combined with results previously obtained for HBr, KBr, NaBr, and NH_3 solutions, to obtain values for the ionization constant of water up to 800 °C and 400 MPa. It turns out that Marshall and Franck significantly used the K_W data obtained by Quist (1970) in their fitting procedure. However, as pointed out by Mesmer *et al.* (1991), the accuracy of these data were limited by the need to use the equilibrium constants that were not available and had to be estimated. Indeed, Quist (1970) made two extrathermodynamic assumptions: (1) the conductance of unhydrolyzed NH_4Br can be set equal to the measured value for KBr at the same ionic strength, and (2) the ionization constant of NH_4Br can be assumed to be equal to the corresponding values for NaBr. As a result, the uncertainty of Quist's results may be larger than that reported in his paper (0.5 l. u.). In the 1970s Lukashov *et al.* (1975) studied the conductivity of solutions of KCl, LiCl, NaOH, KOH, and HCl in water and steam at very low densities from 0.085 to 0.70 $g\,cm^{-3}$, and temperatures and pressures corresponding to the liquid–vapor coexisting state. Those data were used by Svistunov *et al.* (1977) for estimating the ionization constant of water at densities between 0.08 and 0.22 $g\,cm^{-3}$. Also, Svistunov *et al.* (1978) experimentally obtained some additional data close to the critical point of water. The investigations of Lukashov *et al.* (1975) and Svistunov *et al.* (1978) are the only data, besides those of Quist (1970), that provide information about the pK_W at low densities and we have included the data of Svistunov *et al.* (1977, 1978) in our fitting procedure.

Conductance measurements have also been carried out in other extreme regions, namely at very high pressures and temperatures. Holzapfel and Franck (1966) measured the specific conductance of water up to 1000 °C and 10 000 MPa. A shock wave technique used by Hamann and Linton (1969) to measure the conductance of KCl, KOH, and HCl aqueous solutions allowed the authors to attain a pressure of about 13 000 MPa. We have not used the superhigh pressure data in this work due to a possible large experimental uncertainty of the shock wave technique.

More recently, an improved experimental technique and data treatment in the conductivity measurements were employed for obtaining K_W along the water–vapor coexisting curve. Bignold *et al.* (1971) published the conductance data obtained in the saturation region of pure water. Fisher and Barnes (1972) determined pK_W values using the limiting conductances and the ion association constants of aqueous solutions of NH_4OH, HAc, and NH_4Ac at temperatures from 100 to 350 °C.

2.5.2. Potentiometry

In spite of significant progress achieved at the present time, it is sill not easy to obtain the limiting ionic conductances and ion association constants using the conductivity measurements in supercritical water. In general, an uncertainty of about 0.1–0.5 l. u. in pK_W may be ascribed to those values. On the other hand, potentiometry is one of the most precise techniques that can be used to obtain the ionization constant of water. Harned and Robinson (1940) used the potentiometric method in their classical works to measure K_W. Up to now, their results are the most precise data obtained at temperatures below 100 °C. Many investigators have used those data as a reliable reference in the low temperature region and we employ these data in the same way.

At high temperatures, the hydrogen electrode concentration cell was proven to be the best technique for accurate measurements of K_W. The most accurate determination of K_W at elevated temperatures appears to be the potentiometric study of Sweeton *et al.* (1974). For the vapor–liquid coexisting region we took into account the experimental data of Sweeton *et al.* (1974), Percovets and Kryukov (1969), Macdonald *et al.* (1973), and Palmer and Drummond (1988). However, in this region of the water phase diagram we did not take into account the data of Dobson and Thirsk (1971) because their values significantly deviated (about 0.1 l. u.) from the data of all other authors.

The potentiometric measurements were also found to be very effective at high pressures and low temperatures. Using this technique, Hamann (1963) and then Whitfield (1972) determined pK_W at ambient temperatures and high pressures up to 200 MPa. Linov and Kryukov (1972), and Kryukov *et al.* (1980) studied the ionization constant of water up to 800 MPa at temperatures between 18 and 150 °C. All of the papers mentioned above have been taken into account in this work and the experimental data presented in these articles were used in the fitting procedure.

2.5.3. Calorimetry

Calorimetry has been demonstrated as a useful technique for studying the chemical equilibria in aqueous solutions over a wide range of temperatures. An adiabatic calorimeter was used by Ackermann (1958) at temperatures up to 130 °C

TABLE 3. References on the experimentally obtained K_W data used for estimating the empirical parameters given in Tables 1 and 2

No.[a]	Reference	Number of points[b]	Ranges of temperature, pressure, and density	Method[c]	Reported or estimated error in lg K_W (l. u.)	Mean/maximum deviation from calculated by Eq. (39) values (l. u.)
1	Harned and Robinson (1940)	13	sat. curve, $t<60$ °C	Pot.	0.001	0.0015/0.0034
2	Ackermann (1958)	7	sat. curve, $t<130$ °C	Cal.	0.005	0.013/0.060
3*	Hamann (1963)	8	$t=25$ °C, $P<200$ MPa	Pot.	0.01–0.03	0.0033/0.0083
4	Percovets and Kryukov (1969)	6	sat. curve, $t<150$ °C	Pot.	0.02	0.019/0.038
5*	Quist (1970)	31	$t=300$–800 °C, $\rho=0.45$–1.0 g cm^{-3}	Cond.	0.3–0.5	0.33/0.82
6	Bignold *et al.* (1971)	24	sat. curve, $t<271$ °C	Cond.	0.008–0.40	0.018/0.071
7	Fisher and Barnes (1972)	3	sat. curve, $t>250$ °C	Cond.	0.2	0.32/0.50
8*	Whitfield (1972)	40	$t=5$–35 °C, $P<200$ MPa	Pot.	0.005–0.015	0.0034/0.015
9*	Linov and Kryukov (1972)	32	$t=18$–75 °C, $P<800$ MPa	Pot.	0.02–0.03	0.055/0.13
10	Macdonald *et al.* (1973)	8	sat. curve, $t<250$ °C	Pot.	0.01–0.03	0.019/0.050
11*	Sweeton *et al.* (1974)	7	sat. curve, $t<250$ °C	Pot.	0.01	0.0065/0.012
			sat. curve, $t\geqslant 250$ °C		0.02–0.05	0.023/0.038
12	Svistunov *et al.* (1977)	4	$t=330$–370 °C, $\rho=0.08$–0.2 g cm^{-3}	Cond.	0.5–1.0	0.33/0.66
13	Svistunov *et al.* (1978)	12	sat. curve, $t=300$–340 °C	Cond.	0.1–0.2	0.074/0.14
			$t=395$ °C		0.2–0.4	0.10/0.15
14	Kryukov *et al.* (1980)	31	$t=25$–150 °C, $P<600$ MPa	Pot.	0.01–0.04	0.013/0.040
15	Palmer and Drummond (1988)	6	sat. curve, $t<250$ °C	Pot.	0.01	0.014/0.025
16	Chen *et al.* (1994a,b)	5	sat. curve, $t>250$ °C	Cal.	0.02–0.1	0.077/0.23

[a]Data taken into account by Marshall and Franck (1981) are marked by the asterisk.
[b]Number of experimental points taken into account in the fitting procedure.
[c]Cond.=conductivity measurements, Pot.=potentiometry measurements, Cal.=calorimetry measurements.

for measuring the apparent molal heat capacities of aqueous solutions of NaCl, NaOH, and HCl. The water ionization constant was calculated by integrating the obtained experimental data. Precision of the obtained values seems to be comparable to that of the potentiometric studies of Harned and Robinson (1940). Therefore, we included these data in our treatment. Significant improvement of high-temperature solution calorimetry was made in 1980 after developing the flow calorimeter. The high temperature calorimetric data, obtained by Chen *et al.* (1994b), were used in this work. The K_W values of Chen *et al.* (1994b) were derived using the enthalpies of reaction between NaOH(aq) and HCl(aq). The measurements were carried out at temperatures between 250 and 350 °C along the liquid–vapor saturation curve.

In conclusion, Table 3 consists of the references that were taken into account in this work. Only the original experimental data were considered for the fitting procedure. The data taken into account by Marshall and Franck (1981) are marked by the asterisk. The mean and maximum deviations of the data from the results of calculations are also given in Table 3. In Fig. 2, we show the data distribution over ranges of temperature and density studied. The collected data cover the region of temperatures from 0 to 800 °C, densities from 0.1 to 1.2 g cm^{-3}, and pressures from ambient to 800 MPa. The open circles in Fig. 2 represent the data of Holzapfel and Franck (1966) and Hamann and Linton (1969), that were not included in the fitting procedure because of some uncertainties in their experimental procedure.

3. Results and Discussion

The values of pK_W calculated over a wide range of temperature (0–1000 °C) and pressure (0.1–1000 MPa) using Eq. (39) are tabulated in Table 4. The differences between calculated and experimental values of pK_W are compared in Figs. 3 and 4 at low and high densities, respectively, for both Model I [Eq. (45)] and Model II [Eq. (39)], and they were found to be compatible with the corresponding experimental errors (see Table 3). At the liquid-phase region and moderate temperature and pressure ($T<200$ °C, $P<200$ MPa) the deviations of the experimental data from values calculated by Eq. (39) do not generally exceed 0.05 l. u. (except the data of Fisher and Barnes 1972). Most of the other available experimental data do not differ from those predicted by our equations by more than the standard deviation obtained 0.16 l. u. with the exception of the data of Quist (1970) and Svistunov *et al.* (1977). The significant deviations (up to 0.8 l. u.) in the

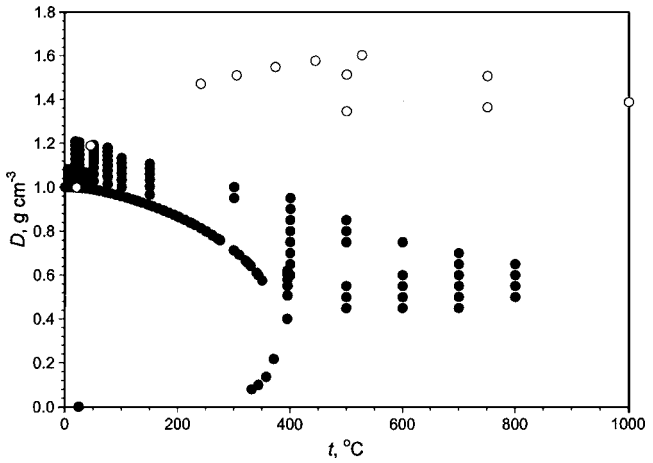

FIG. 2. Temperature–density distribution of the available experimental K_W data: (●) selected points, (○) rejected points.

TABLE 4. Negative logarithm (base 10) of the ionization constant of water, K_W, calculated using Model II [Eq. (39)]

	Temperature (°C)								
Pressure (MPa)	0	25	50	75	100	150	200	250	300
0.1 MPa or saturated pressure[a]	14.95	13.99	13.26	12.70	12.25	11.64	11.31	11.20	11.34
25	14.85	13.91	13.18	12.61	12.17	11.54	11.19	11.05	11.12
50	14.75	13.82	13.10	12.53	12.08	11.45	11.08	10.90	10.89
75	14.66	13.74	13.03	12.46	12.01	11.36	10.97	10.77	10.71
100	14.58	13.67	12.95	12.39	11.93	11.28	10.88	10.65	10.57
150	14.42	13.52	12.82	12.25	11.79	11.13	10.71	10.46	10.33
200	14.28	13.39	12.69	12.12	11.67	11.00	10.56	10.29	10.13
250	14.14	13.27	12.57	12.00	11.55	10.88	10.43	10.14	9.96
300	14.02	13.15	12.45	11.89	11.44	10.76	10.31	10.01	9.81
350	13.91	13.04	12.35	11.79	11.33	10.65	10.19	9.88	9.68
400	13.80	12.93	12.24	11.69	11.23	10.55	10.08	9.77	9.55
500	13.59	12.74	12.05	11.50	11.04	10.36	9.88	9.56	9.33
600	13.41	12.56	11.87	11.32	10.87	10.18	9.70	9.37	9.13
700	13.24	12.39	11.71	11.16	10.71	10.02	9.54	9.20	8.96
800	13.08	12.23	11.56	11.01	10.55	9.86	9.38	9.04	8.79
900	12.93	12.09	11.41	10.86	10.41	9.72	9.24	8.89	8.64
1000	12.79	11.95	11.27	10.72	10.27	9.58	9.10	8.75	8.49
	Temperature (°C)								
	350	400	450	500	600	700	800	900	1000
0.1 MPa or saturated pressure[a]	11.92	—	—	—	—	—	—	—	—
25	11.55	16.57	18.13	18.76	19.43	19.83	20.11	20.31	20.41
50	11.08	11.56	12.71	14.20	15.62	16.28	16.69	16.98	17.18
75	10.80	11.05	11.49	12.16	13.51	14.30	14.79	15.13	15.37
100	10.60	10.74	11.00	11.38	12.30	13.04	13.54	13.90	14.16
150	10.30	10.34	10.46	10.64	11.12	11.61	12.03	12.36	12.61
200	10.06	10.06	10.12	10.22	10.51	10.85	11.17	11.44	11.66
250	9.87	9.84	9.86	9.92	10.11	10.36	10.61	10.83	11.02
300	9.70	9.65	9.65	9.68	9.81	10.00	10.20	10.39	10.55
350	9.55	9.49	9.46	9.48	9.57	9.71	9.88	10.04	10.18
400	9.42	9.34	9.31	9.30	9.36	9.48	9.61	9.75	9.88
500	9.18	9.09	9.03	9.01	9.02	9.09	9.19	9.30	9.40
600	8.97	8.87	8.80	8.76	8.75	8.79	8.86	8.94	9.03
700	8.79	8.67	8.59	8.55	8.51	8.54	8.59	8.65	8.72
800	8.62	8.49	8.41	8.35	8.31	8.31	8.35	8.41	8.47
900	8.46	8.33	8.24	8.18	8.12	8.12	8.14	8.19	8.24
1000	8.31	8.18	8.08	8.02	7.95	7.94	7.96	7.99	8.04

[a]0.1 MPa at $t<100\,^{\circ}\mathrm{C}$, and saturation pressure for $t>100\,^{\circ}\mathrm{C}$.

low density and supercritical regions may be due to large experimental errors at these state parameters. Nevertheless, our formulation satisfactorily fits the low density data of Svistunov *et al.* (1977) for $D<0.4\ \mathrm{g\,cm^{-3}}$, while the M&F equation does not, and the calculated values may differ from experimental data up to 4 l. u. in this region. The standard deviation of the collected experimental data from that calculated using the M&F equation is 0.49 l. u., that is three times larger than the deviation from Eq. (39) (0.16 l. u.). Note that the largest contribution to the deviations between the M&F and observed data give the low-density data of Svistunov *et al.* (1977). It is also interesting to note that in spite of the fact that we did not used the high-pressure values, Eq. (3.9) reproduces the data of Holzapfel and Franck (1966) up to 10 000 MPa $1.5\ \mathrm{g\,cm^{-3}}$, and the data of Hamann and Linton (1969) up to 13 000 MPa $1.7\ \mathrm{g\,cm^{-3}}$ within 1.5 l. u. This fact demonstrates a significant predictive capability of our equation due to a theoretical background that was used in our approach.

Analysis of the fitting results at the saturated vapor pressure is shown in Fig. 5. When $D>0.8\ \mathrm{g\,cm^{-3}}$ the deviation of our data from those of Sweeton *et al.* (1974) is generally less than 0.01 l. u. Also, our results are practically coincident with those of Marshall and Franck at the saturation curve up to 275 °C (Fig. 5) using both Models I and II. However, at temperatures above 275 °C, the difference between M&F and Eq. (39) is pronounced and can be as much as 0.4 l. u. at a temperature of 350 °C.

An isochoric plot of $\mathrm{p}K_W$, as a function of inverse tem-

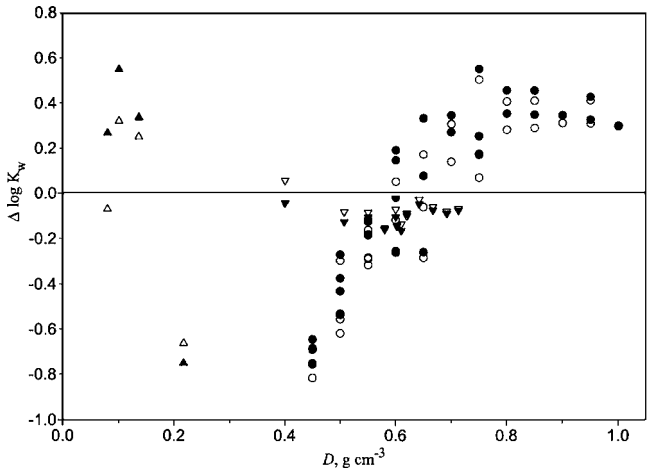

FIG. 3. Deviation of calculated lg K_W values from experimental data in supercritical and low-density regions at $0.08 \leqslant D \leqslant 1.00$ g cm^{-3}: (○) Quist (1970), (△) Svistunov *et al.* (1977), and (▽) Svistunov *et al.* (1978). Deviation from Model I are shown by filled symbols and deviation from Model II are shown by open symbols.

perature ($1/T$), was calculated using Model II and the M&F equation for densities of 1.0, 0.7, 0.4, and 0.4 g cm^{-3} and is shown in Fig. 6. All graphs are close to a straight line over a wide temperature range. In the first case ($D = 1.0$ g cm^{-3}) our calculations almost completely coincide with the M&F's result. However, the difference between our approach and M&F's model becomes more pronounced if density decreases and reaches 4 l. u. at 0.1 g cm^{-3}.

In Fig. 7 we compare the density dependence of pK_W calculated using our model (Models I and II are indistinguishable in figure scale) and the M&F equation at 400 and 800 °C. From this figure we can see that a significant deviation between two formulations begins to occur at a density of 0.6 g cm^{-3}. In Fig. 8 we present the same density dependence in logarithmic scale to show the limiting behavior of the regarded models. Additionally, in this figure we plot (at 400 °C) the calculated values using M&F Eq. (40) and the modified M&F Eq. (42) in which the zero-density limit is correct. The calculated data from the modified M&F Eq. (42) are higher (in absolute values) than our data carried out using Eq. (39). The fact that the M&F equation overestimates the

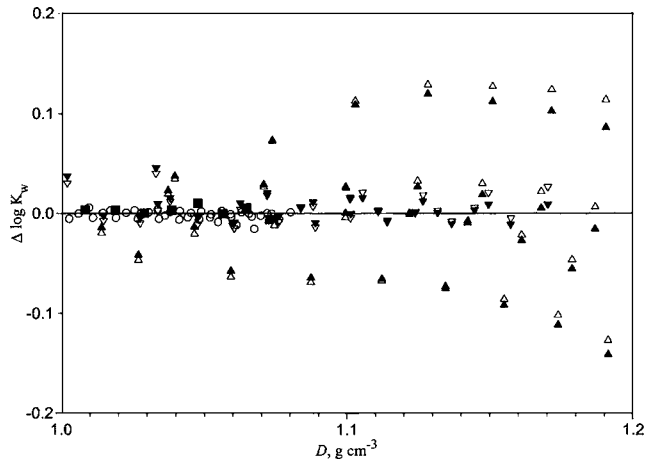

FIG. 4. Deviation of calculated lg K_W values from the experimental data in high-density region at $1.0 \leqslant D \leqslant 1.2$ g cm^{-3}: (○) Whitfield (1972), (□) Hamann (1963), (△) Linov and Kryukov (1972), (▽) Kryukov *et al.* (1980). Deviation from Model I are shown by filled symbols and from Model II—by open symbols. For better appearance the Hamann's deviations are given only for Model I, and Whitfield's—only for Model II.

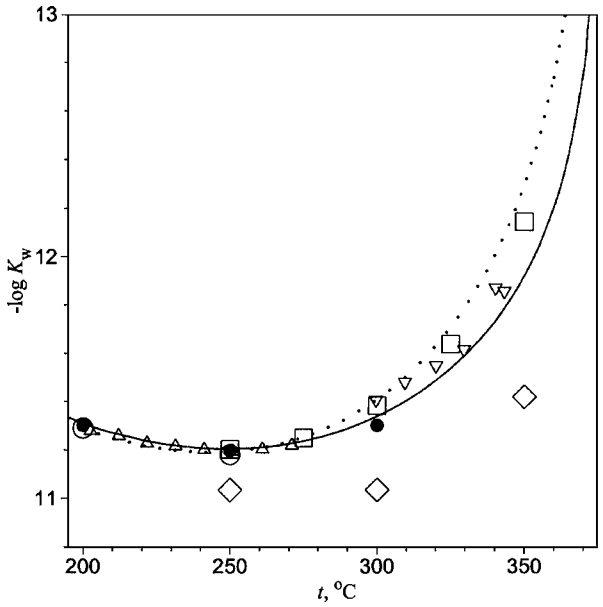

FIG. 5. Temperature dependence of lg K_W at the saturated vapor pressure for $T \geqslant 200$ °C: (· · · ·) Marshall and Franck (1981), (——) Model II [Eq. (39)]. High temperature experimental data: (△) Bignold *et al.* (1971), (◇) Fisher and Barnes (1972), (●) Sweeton *et al.* (1974), (▽) Svistunov *et al.* (1978), (○) Palmer and Drummond (1988), (□) Chen *et al.* (1994a, b).

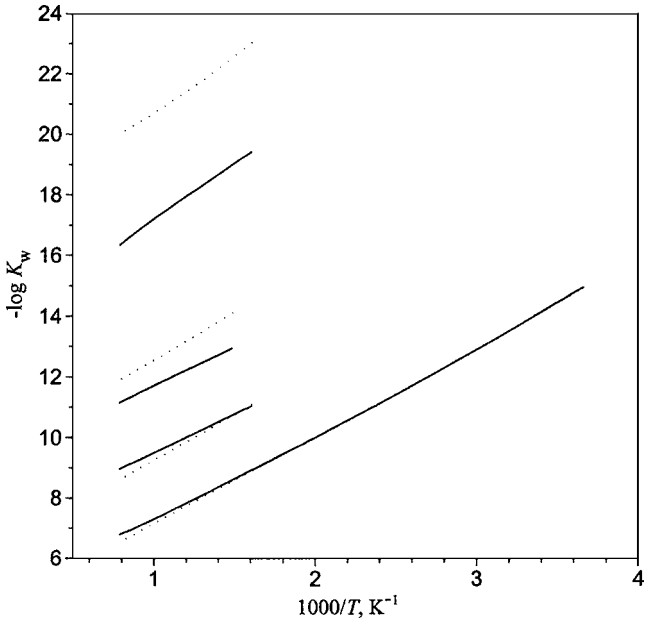

FIG. 6. Temperature dependence of lg K_W at a constant density: (· · · ·) Marshall and Franck (1981), (——) Model II [Eq. (39)]. Curves from bottom to top correspond to densities as follows: 1.0, 0.7, 0.4, and 0.1 g cm^{-3}.

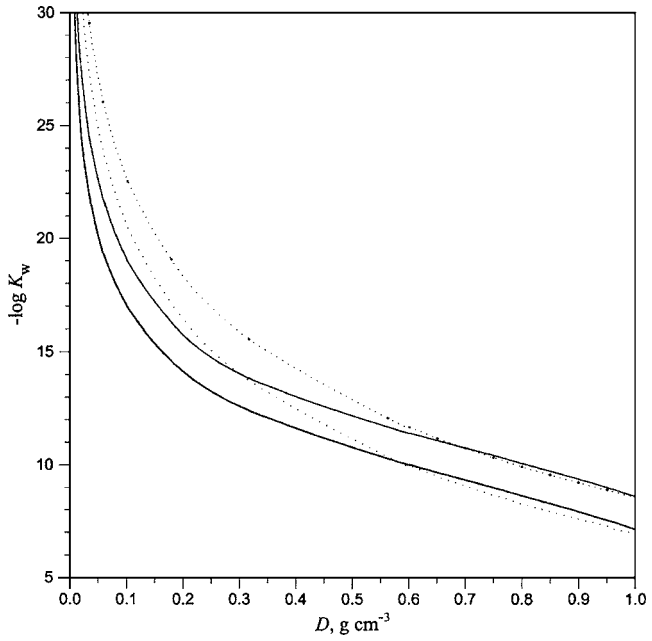

FIG. 7. Density dependence of lg K_W at 400 °C (upper curves) and 800 °C (lower curves): (· · · ·) Marshall and Franck (1981), (——) Model II [Eq. (39)].

absolute values of pK_W at low densities has been reported elsewhere (Chen *et al.* 1994a), and we confirm the conclusion made in this paper based on the results of our study. Indeed, the agreement between pK_W of Sweeton *et al.* (1974) and those calculated using the M&F equation is excellent only up to about 250 °C, but as temperature increases, the pK_W values estimated by the M&F formulation increase more rapidly than the potentiometric results of Sweeton *et al.* (1974), the conductivity data of Svistunov *et al.* (1978), and the calorimetric results of Chen *et al.* (1994b) (see Fig. 5). The M&F formulation is also in contradiction with the theoretical results of Pitzer (1982) who came to the conclusion that the M&F equation underestimates the true values of pK_W at low densities and overestimates it at very low (less than 10^{-3} g cm^{-3}) densities. According to the approach developed by Tanger and Pitzer (1989a, b), pK_W should increase more rapidly than M&F predicts at densities from 0.4 down to approximately 10^{-3} g cm^{-3}, and then it should intersect the M&F curve, approaching the gas phase limiting value. Our formulation approaches the same gas phase limit as Pitzer's model does (Fig. 8); however our formulation generally remains under the M&F curve in the low-density range. It is clear that both the additional experimental measurements and theoretical studies are needed to provide a correct description of pK_W behavior in the low-density region.

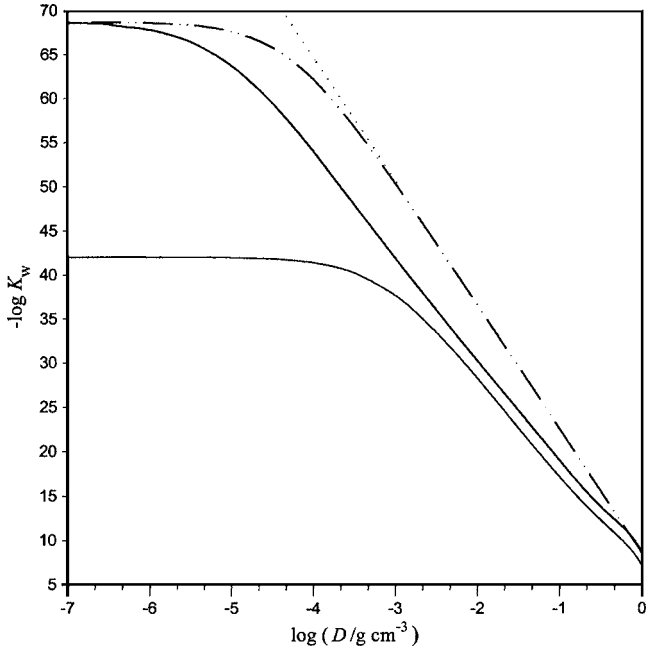

FIG. 8. Dependence of lg K_W from lg(D/g cm^{-3}) at 400 and 800 °C: (· · · ·) Marshall and Franck (1981) [Eq. (40)], 400 °C; (—·—·—·—) modified Marshall and Franck equation [Eq. (42)], 400 °C; (——) Model II [Eq. (39)], 400 °C (upper curve) and 800 °C (lower curve).

4. Acknowledgments

The authors gratefully acknowledge support of this work by the International Association for the Properties of Water and Steam and National Science Foundation (Grant No. EAR 9725191).

5. Appendix

According to the Bragg–Williams adsorption theory (Hill 1956; Lopatkin 1983) the occupation fraction obeys the following equations:

$$z(\theta) = \theta(1-\theta)^{-1} \exp(\omega\theta/RT), \tag{A1}$$

$$\Delta\tilde{\mu} = \frac{\mu_I^S}{RT} = n\left[\theta \ln\frac{\theta}{z} + (1-\theta)\ln(1-\theta) + \frac{\omega\theta^2}{2RT}\right]. \tag{A2}$$

To obtain the approximate expression for θ we consider a trial function as follows:

$$\Theta(z) = \frac{1}{2} + \frac{1}{2ab}\ln\left\{\frac{\cosh[a(\ln z + c)]}{\cosh[a(\ln z + c - b)]}\right\}, \tag{A3}$$

where a, b, and c are the parameters to be determined. This function reproduces qualitatively the dependence of θ from z and has the true limiting values at $\ln z \to \pm\infty$. Then, we assume that quantitative agreement would be better if the following conditions are satisfied: (1) correct limiting behavior of the derivative $\partial\Delta\tilde{\mu}/\partial \ln z$ at $z \to \infty$; (2) correct value of z at $\theta = 1/2$; and (3) precise value of the derivative $\partial\theta/\partial \ln z$ at $\theta = 1/2$. To find the appropriate equations for parameters a, b, and c we should start with the general relation:

$$\frac{\partial\Delta\tilde{\mu}}{\partial \ln z} = \frac{\partial\Delta\tilde{\mu}}{\partial\theta}\frac{\partial\theta}{\partial \ln z}. \tag{A4}$$

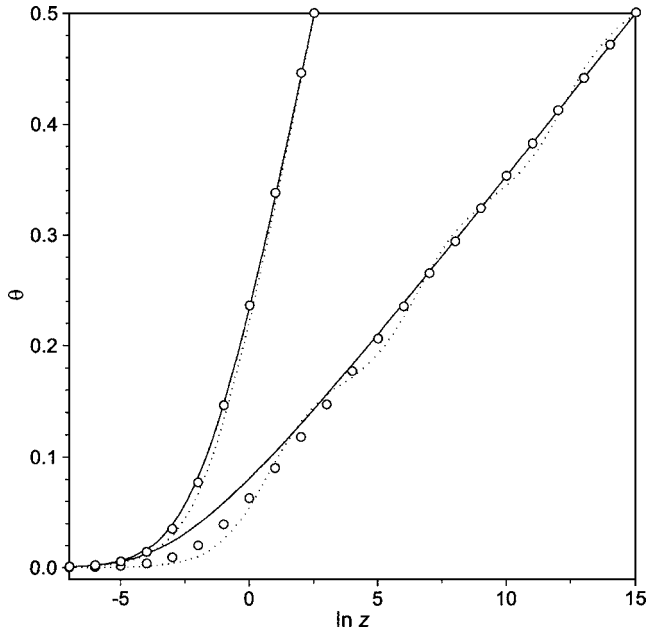

FIG. 9. Bragg–Williams sorption isotherm, $\theta=\theta(z)$, calculated using different values of $\omega/RT=5$ (left curves) and $\omega/RT=30$ (right curves): (——) macroscopic approximation [Eq. (A1)], (· · · ·) exact summation [Eq. (A18)] for $n=6$, (○) our approximation [Eq. (A15)].

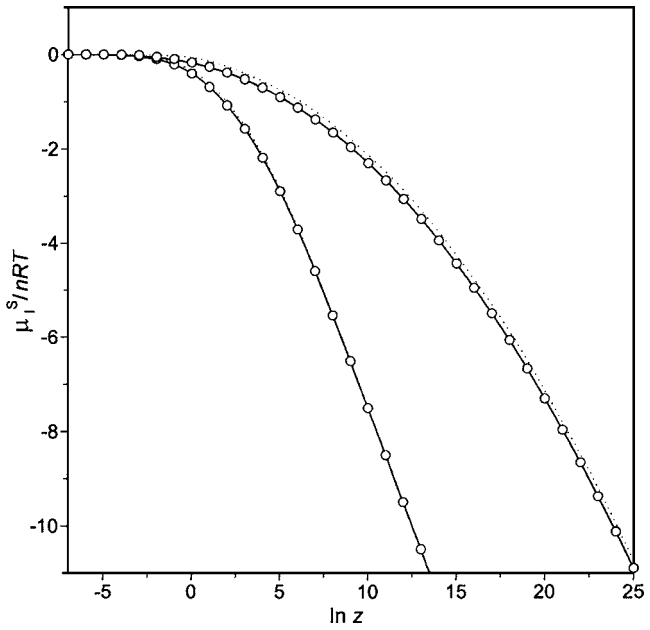

FIG. 10. Excess chemical potential $\Delta\tilde{\mu}$ of the sorbent particle in the Bragg–Williams approximation calculated using different values of $\omega/RT=5$ (left curve) and $\omega/RT=30$ (right curve): (——) macroscopic approximation [Eqs. (A1) and (A2)], (· · · ·) exact summation [Eq. (A17)] for $n=6$, (○) our approximation [Eqs. (A2) and (A15)].

Then, by taking into account the original Bragg–Williams sorption isotherm, we can write:

$$\frac{\partial\Delta\tilde{\mu}}{\partial\theta}=-n\left(\frac{1}{1-\theta}+\frac{\omega\theta}{RT}\right), \tag{A5}$$

$$\frac{\partial\theta}{\partial\ln z}=\left(\frac{1}{\theta}+\frac{1}{1-\theta}+\frac{\omega}{RT}\right)^{-1}, \tag{A6}$$

$$\left.\frac{\partial\theta}{\partial\ln z}\right|_{\theta=1/2}=\left(4+\frac{\omega}{RT}\right)^{-1}, \tag{A7}$$

$$\ln z(1/2)=\omega/2RT, \tag{A8}$$

$$\lim_{z\to\infty}\frac{\partial\Delta\tilde{\mu}}{\partial\ln z}=-n. \tag{A9}$$

For simplicity, let us introduce new quantities: $x=a(\ln z+c)$, and $y=a(\ln z+c-b)$. After substituting Eq. (A3) into Eqs. (A4)–(A6) we can get:

$$\partial\Theta/\partial\ln z=(\tanh x-\tanh y)/2b, \tag{A10}$$

$$\begin{aligned}\lim_{z\to\infty}\frac{\partial\Delta\tilde{\mu}}{\partial\ln z}&=-n\lim_{\substack{z\to\infty\\ \Theta\to 1}}\left[\frac{1+\Theta(1-\Theta)\omega/RT}{1-\Theta}\frac{\partial\Theta}{\partial\ln z}\right]\\ &=-na\lim_{z\to\infty}\left[\frac{\tanh x-\tanh y}{2ab-(\ln\cosh x-\ln\cosh y)}\right]\\ &=na\lim_{z\to\infty}\left[\frac{\operatorname{sech}^2 x-\operatorname{sech}^2 y}{\tanh x-\tanh y}\right]\\ &=-na\lim_{z\to\infty}(\tanh x+\tanh y)=-2na.\end{aligned} \tag{A11}$$

Hence, taking into account Eq. (A9) we found that $a=1/2$. The second condition expressed by Eq. (A8) will obviously be satisfied if $x=-y$ for $z=\exp(\omega/2RT)$, therefore

$$c+\omega/2RT=b-c-\omega/2RT. \tag{A12}$$

Further, it follows from the last two relations obtained and from Eq. (A10) that

$$\left.\frac{\partial\Theta}{\partial\ln z}\right|_{\theta=1/2}=\frac{1}{2b}(\tanh x-\tanh y)\Big|_{\theta=1/2}=\frac{1}{b}\tanh\frac{b}{4}. \tag{A13}$$

Equating the right-hand sides of Eqs. (A7) and (A13) we have:

$$(4+\omega/RT)^{-1}=b^{-1}\tanh(b/4). \tag{A14}$$

For sufficiently large ω, parameter b should be much greater than unity, and consequently, $\tanh(b/4)$ becomes close to 1. For example, if $\omega/RT=4$, $b\approx 7.66$, and $\tanh(b/4)\approx 0.96$. Practically, in the case of formation of an ion–molecular complex, the value of ω/RT has an order between 10 and 50 (Kebarle 1977). Therefore, assuming that $\omega>5RT$ we may put $b=\omega/RT+4$, and as a consequence, from Eq. (A12) we can get the parameter c being equal to 2.0. Using the received values of a, b, and c we obtain the desired expression as

$$\theta=\Theta(z)=\frac{1}{2}+\frac{1}{\frac{\omega}{RT}+4}\ln\left[\frac{\cosh\left(\frac{\ln z}{2}+1\right)}{\cosh\left(\frac{\ln z}{2}-\frac{\omega}{2RT}-1\right)}\right]. \tag{A15}$$

In Fig. 9, we compare the developed approximation with a numeric solution of Bragg–Williams macroscopic equations [Eqs. (A1) and (A2)] for two particular values of ω: (1) $5RT$ and (2) $30RT$. Also, in this figure we show the results obtained by the exact summation using the grand partition function Ξ_n for $n=6$:

$$\Xi_n=\sum_{i=0}^{n}\frac{n!}{i!(n-i)!}z^i\exp\left(\frac{-i^2\omega}{2nRT}\right), \tag{A16}$$

$$\Delta\tilde{\mu}=-\ln\Xi_n, \tag{A17}$$

$$\theta(z)=\frac{\sum_{i=0}^{n}\frac{n!i}{i!(n-i)!}z^i\exp\left(\frac{-i^2\omega}{2nRT}\right)}{n\Xi_n}. \tag{A18}$$

All three curves are symmetrical with respect to the point $\theta=1/2$, so we show only a half of the graphs. The exact and approximate summations are proved to be very close to each other. The stair-like shape is only slightly distinguishable for the curve obtained using the direct summation [Eq. (A18)], with a number of steps being equal to n. It is a remarkable fact that the microscopic result for such a small value of n $(=6)$ becomes very close to the macroscopic approximation which, strictly speaking, is only valid at $n\to\infty$. As illustrated in Fig. 9, the proposed approximation well reproduces both the macroscopic and exact result. In Fig. 10 we show the relationship between $\Delta\tilde{\mu}$ and $\ln z$. It should be noted that this result was obtained by substituting Eq. (A15) into Eq. (A2). Referring to Fig. 10, the agreement between all three models is excellent and, therefore, we have employed Eq. (A15) together with Eq. (A2) in our calculations of μ_I^s.

6. References

Ackermann, Th., "Aussagen über die eigendissoziation des wassers aus molwarmemessungen gelöster elektrolyte," Z. Elektrochem. **62**, 411 (1958).

Bandura, A. V., and S. N. Lvov, "The ionization constant of water over a wide range of temperatures and densities" in: *Steam, Water, and Hydrothermal Systems: Physics and Chemistry. Meeting the Needs of Industry*, edited by P. R. Tremaine, P. G. Hill, D. E. Irish, and P. V. Balakrishnan (NRC Press, Ottawa, 2000), pp. 96–103.

Ben-Naim, A., *Solvation Thermodynamics* (Plenum, New York, 1987).

Bignold, G. J., A. D. Brewer, and B. Hearn, "Specific conductivity and ionic product of water between 50 and 271 °C," Trans. Faraday Soc. **67**, 2419 (1971).

Born, M., "Volumen und Hydrationswarme der Ionen," Z. Phys. **1**, 45 (1920).

Chase, M. W., *JANAF Thermochemical Tables*, 4th ed., J. Phys. Chem. Ref. Data, Monograph 9 (1998).

Chen, X., R. M. Izatt, and J. L. Oscarson, "Thermodynamic data for ligand interaction with protons and metal ions in aqueous solutions at high temperatures," Chem. Rev. **94**, 467 (1994a).

Chen, X., J. L. Oscarson, S. E. Gillespie, H. Cao, and R. M. Izatt, "Determination of enthalpy of ionization of water from 250 to 350 °C," J. Solution Chem. **23**, 747 (1994b).

Dobson, J. V., and H. R. Thirsk, "Determination of the ionization constant of water between 100 to 200 °C by emf measurements, with some derived thermodynamic quantities," Electrochim. Acta **16**, 315 (1971).

Fernández-Prini, R. J., H. R. Corti, and M. L. Japas, *High-Temperature Aqueous Solutions: Thermodynamic Properties* (CRC, Boca Raton, FL, 1992).

Fisher, J. R., and H. L. Barnes, "The ion-product constant of water to 350°," J. Phys. Chem. **76**, 90 (1972).

Garisto, F., P. G. Kusalik, and G. N. Patey, "Solvation energy of ions in dipolar solvents," J. Chem. Phys. **79**, 6294 (1983).

Hamann, S. D., "The ionization of water at high pressures," J. Phys. Chem. **67**, 2233 (1963).

Hamann, S. D., and M. Linton, "Electrical conductivities of aqueous solutions of KCl, KOH and HCl, and the ionization of water at high shock pressures," Trans. Faraday Soc. **65**, 2186 (1969).

Harned, H. S., and R. A. Robinson, "A note on the temperature variation of the ionization constants of weak electrolytes," Trans. Faraday Soc. **36**, 973 (1940).

Harvey, A. H., A. P. Peskin, and S. A. Klein, *NIST/ASME Steam. Formulation for General and Scientific Use*, NIST Standard Reference Database 10, Version 2.21 (National Institute of Standards and Technology, Gaithersburg, MD, 2000).

Hill, T. L., *Statistical Mechanics* (McGraw–Hill, New York, 1956).

Holzapfel, W. B., and E. U. Franck, "Conductance and ionic dissociation of water to 1000 °C and 100 kbar," Ber. Bunsenges. Phys. Chem. **70**, 1105 (1966).

Kebarle, P., "Ion thermochemistry and solvation from gas phase ion equilibria," Ann. Rev. Phys. Chem. **28**, 445 (1977).

Klots, C. S., "The pH of steam," J. Phys. Chem. **88**, 4407 (1984).

Kryukov, P. A., L. I. Starostina, and E. G. Larionov, "Ionization of water at pressures from 1 to 6000 bar and temperatures from 25 to 150 °C," *Water and Steam* (Pergamon, New York, 1980), p. 513.

Lau, Y. K., S. Ikuta, and P. Kebarle, "Thermodynamics and kinetics of the gas-phase reactions: $H_3O^+(H_2O)_{n-1}+H_2O=H_3O^+(H_2O)_n$," J. Am. Chem. Soc. **104**, 1462 (1982).

Lee, L. L., *Molecular Thermodynamics of Nonideal Fluids* (Butterworths, Boston, 1988).

Linov, E. D., and P. A. Kryukov, "Ionization of water at pressures up to 8000 kgf/cm^2 and temperatures 18, 25, 50, and 75 °C," Izv. SO AN SSSR, Ser. Khim. Nauk (Russ.) No. **4**, 10 (1972).

Lopatkin, A. A., *Theoretical Foundation of Physical Adsorption* (MSU, Moscow, 1983) (in Russian).

Lukashov, Yu. M., K. B. Komissarov, B. P. Golubev, S. N. Smirnov, and E. P. Svistunov, "Experimental investigation of ionic properties of 1:1 electrolytes at high state parameters," Teploenergetica (Russ) **22**, 78 (1975).

Macdonald, D. D., P. Butler, and D. Owen, "High temperature aqueous electrolyte concentration cells and the ionization of liquid water to 200 °C," Can. J. Chem. **51**, 2590 (1973).

Marshall, W. L., and E. U. Franck, "Ion product of water substance, 0–1000 °C, 1–10,000 bars. New international formulation and its background," J. Phys. Chem. Ref. Data **10**, 295 (1981).

Mesmer, R. E., D. A. Palmer, and J. M. Simonson, "Ion association at high temperatures and pressures," in: *Activity Coefficients in Electrolyte Solutions*, 2nd ed., edited by K. S. Pitzer (CRC, Boca Raton, 1991), Chap. 8, p. 491.

Noyes, A. A., Y. Kato, and R. B. Sosman, "The hydrolysis of ammonium acetate and the ionization of water at high temperatures," J. Am. Chem. Soc. **32**, 159 (1910).

Ono, S., and S. Kondo, *Molecular Theory of Surface Tension in Liquids* (Springer, Berlin, 1960).

Palmer, D. A., and S. E. Drummond, "The molal dissociation quotients of water in sodium trifluoromethanesulfonate solutions to high temperatures," J. Solution Chem. **17**, 153 (1988).

Percovets, V. D., and P. A. Kryukov, "Ionization constant of water at temperatures up to 150 °C," Izv. SO AN SSSR, Ser. Khim. Nauk, (Russ.) No. **3**, 9 (1969).

Pitzer, K. S., "Self-ionization of water at high temperature and thermodynamic properties of ions," J. Phys. Chem. **86**, 4704 (1982).

Quist, A. S., "The ionization constant of water to 800° and 4000 bars," J. Phys. Chem. **74**, 3396 (1970).

Quist, A. S., and W. L. Marshall, "Electrical conductances of aqueous sodium bromide solutions from 0 to 800° and at pressures to 4000 bars," J. Phys. Chem. **72**, 2100 (1968).

Reiss, H., "Scaled particle methods in the statistical thermodynamics of fluids," Adv. Chem. Phys. **9**, 1 (1965).

Robinson, R. A., and R. H. Stokes, *Electrolyte Solutions*, 2nd ed. (Butterworth, London, 1965).

Svistunov, E. P., B. P. Golubev, S. N. Smirnov, and V. P. Sevastjanov, ''Ionic product for water for wide range of state parameters,'' Teploenergetika (Russ.) **25**, 70 (1978).

Svistunov, E. P., S. N. Smirnov, and K. B. Komissarov, ''Ionic distribution factors of electrolytes and the ionic product of water at the saturation line,'' Teploenergetika (Russ.) **24**, 63 (1977).

Sweeton, F. H., R. E. Mesmer, and C. F. Baes, Jr., ''Acidity measurements at elevated temperatures. VII. Dissociation of water,'' J. Solution Chem. **3**, 191 (1974).

Tanger, J. C., IV, and K. S. Pitzer, ''Calculation of the ionization constant of H_2O to 2273 K and 500 MPa,'' AIChE J. **35**, 1631 (1989a).

Tanger, J. C., IV, and K. S. Pitzer, ''Calculation of the thermodynamic properties of aqueous electrolytes to 1000 °C and 5000 bar from a semicontinuum model for ion hydration,'' J. Phys. Chem. **93**, 4941 (1989b).

Tawa, G. J., and L. R. Pratt, ''Theoretical calculation of the water ion product K_W,'' J. Am. Chem. Soc. **117**, 1625 (1995).

Wagner, W., and A. Pruß, ''The IAPWS formulation 1995 for the thermodynamic properties of ordinary water substance for general and scientific use,'' J. Phys. Chem. Ref. Data **31**, 387 (2002).

Whitfield, M., ''Self-ionization of water in dilute sodium chloride solution from 5–35 °C and 1–2000 bars,'' J. Chem. Eng. Data **17**, 124 (1972).